

Effects of (–)-epigallocatechin-3-gallate, the main component of green tea, on the cloned rat brain Kv1.5 potassium channels

Bok Hee Choi, Jin-Sung Choi, Do Sik Min, Shin Hee Yoon, Duck-Joo Rhie,
Yang-Hyeok Jo, Myung-Suk Kim, Sang June Hahn*

Department of Physiology, The Catholic University of Korea, College of Medicine, 505 Banpo-dong, Socho-gu, Seoul 137-701, Korea

Received 15 January 2001; accepted 9 April 2001

Abstract

The interaction of (–)-epigallocatechin-3-gallate (EGCG), the main component of green tea (*Camellia sinensis*), with rat brain Kv1.5 channels (rKv1.5) stably expressed in Chinese hamster ovary (CHO) cells was investigated using the whole-cell patch-clamp technique. EGCG inhibited rKv1.5 currents at +50 mV in a concentration-dependent manner, with an IC_{50} of $101.2 \pm 6.2 \mu\text{M}$. Pretreatment with protein tyrosine kinase (PTK) inhibitors (10 μM genistein, 100 μM AG1296), a tyrosine phosphatase inhibitor (500 μM sodium orthovanadate), or a protein kinase C (PKC) inhibitor (10 μM chelerythrine) did not block the inhibitory effect of EGCG on rKv1.5. The inhibition of rKv1.5 by EGCG displayed voltage-independence over the full activation voltage range positive to +10 mV. EGCG had no effect on the midpoint potential or the slope factor for steady-state activation and inactivation. EGCG did not affect the ion selectivity of rKv1.5. The activation (at +50 mV) kinetics was significantly slowed by EGCG. During repolarization (at –40 mV), EGCG also slowed the deactivation of the tail currents, resulting in a crossover phenomenon. Reversal of inhibition was detected by the application of repetitive depolarizing pulses and of identical double pulses, especially during the early part of the activating pulse, in the presence of EGCG. EGCG-induced inhibition of rKv1.5 showed identical affinity between EGCG and the multiple closed states of rKv1.5. These results suggest that EGCG interacts directly with rKv1.5 channels. Furthermore, by analyzing the kinetics of the interaction between EGCG and rKv1.5, we conclude that the inhibition of rKv1.5 channels by EGCG includes at least two effects: EGCG preferentially binds to the channel in the closed state, and blocks the channel by pore occlusion while depolarization is maintained. © 2001 Elsevier Science Inc. All rights reserved.

Keywords: rKv1.5; EGCG; Green tea; Reversal of inhibition

1. Introduction

Green tea (*Camellia sinensis*) is one of the most popular beverages in the world. Because of its many scientifically proven beneficial effects on human health, it has received much attention. The protective effects of green tea against cardiovascular disease, which are induced by lowering blood lipid levels, inhibiting the oxidation of low-density lipoproteins, and inhibiting inflammatory reactions, are well documented [1,2]. Furthermore, green tea has been reported to possess both anticarcinogenic and antitumor activities

[3–6]. Green tea components also play an important role as scavengers of harmful radicals [7,8], and as antioxidants [9,10].

Green tea contains characteristic polyphenolic compounds, commonly known as catechins: (–)-epigallocatechin-3-gallate (EGCG), (–)-epigallocatechin, (–)-epicatechin-3-gallate, and (–)-epicatechin. These compounds account for up to 30–42% of the dry weight [11]. Because EGCG is the main constituent of tea catechins, this compound has recently been investigated experimentally. Several studies have shown the molecular mechanisms of EGCG in many biological functions. EGCG inhibits PKC and protein phosphatase 2A activation via the interaction of EGCG with the phospholipid bilayer of the membrane [12]. EGCG is a selective inhibitor of tyrosine phosphorylation of PDGF-R β and its downstream signaling pathway [13]. These results indicate that EGCG may induce its recognized beneficial effects via a number of different mechanisms.

* Corresponding author. Tel.: +1-82-2-590-1170; fax: +1-82-2-532-9575.

E-mail address: sjhahn@cmc.cuk.ac.kr (S.J. Hahn).

Abbreviations: rKv1.5, rat brain Kv1.5; EGCG, (–)-epigallocatechin-3-gallate; CHO, Chinese hamster ovary; PKC, protein kinase C; PDGF, platelet-derived growth factor; and PTK, protein tyrosine kinase.

To our knowledge, little is known about the interaction of EGCG with any ion channel. Recent studies report that ion channels, especially K^+ channels, are required for cell proliferation. For example, ATP-sensitive K^+ channels are required for the progression of MCF-7 human breast cancer cells through G1 phase [14]. Furthermore, a voltage-gated K^+ channel activity modulates Ca^{2+} influx in colon cancer cells, and subsequently modulates the proliferation of carcinoma cells in colon cancer [15]. Therefore, it is possible that EGCG induces various effects, including anticarcinogenic and antitumor activities, via a mechanism involving direct or indirect interaction between the drug and ion channels, especially K^+ channels. We have used the voltage-gated K^+ channel rKv1.5, expressed in CHO cells, to study its interaction with EGCG because this expression system, using a specific cloned channel, provides an important tool for the study of the pharmacological characteristics of ion channels.

The present study was undertaken to examine the effects of EGCG on rKv1.5 channels, to explore the mechanisms of EGCG action using the whole-cell patch-clamp technique, and to find a candidate mechanism with which to explain the various beneficial effects of EGCG.

2. Materials and methods

2.1. Cell culture

The method for establishing rKv1.5 expression in CHO cells has been previously described in detail [16]. Briefly, rKv1.5 cDNA [17] was subcloned into the expression vector pCR3.1 (Invitrogen Corporation), and transfected into CHO cells using FuGENE6 (Boehringer Mannheim). Stable transfectants were selected by subculturing in the presence of G418 (Life Technologies). Cells were cultured in Iscove's modified Dulbecco's medium (IMDM, Life Technologies) supplemented with 10% fetal bovine serum, 0.1 mM hypoxanthine, 0.01 mM thymidine, and 500 μ g/mL of G418. The cultures were passaged every 2–3 days, using a brief trypsin/EDTA treatment. The trypsin/EDTA-treated cells were seeded onto glass coverslips (12-mm diameter; Fisher Scientific) in a Petri dish 24 hr before use. Coverslips with attached cells were transferred to a continually perfused recording chamber (RC-13, Warner Instrument Corporation) for the electrophysiological experiments.

2.2. Electrophysiological recordings

All experiments were carried out at room temperature (22–23°). The rKv1.5 current was measured using the whole-cell configuration of the patch-clamp technique [18]. An Axopatch 1D patch-clamp amplifier (Axon Instruments) was used for whole-cell clamping. Micropipettes, fabricated from PG10165-4 glass capillary tubing (World Precision Instruments) using a vertical puller (model PP-83, Narish-

ige), had a tip resistance of 2–3 M Ω when filled with the internal pipette solution. Liquid junction potentials between the external and pipette solutions were zeroed, and the micropipettes were gently lowered onto the cells to form gigaohm seals by suction. After pipette capacitance compensation, cells were ruptured with brief additional suction. Analog capacity compensation and 80% series resistance compensation were used in all whole-cell measurements. Leak subtraction was not used in this study. The sampling rate was 5 kHz, and currents were low-pass filtered at 2 kHz (four-pole Bessel filter) before being digitized and stored on an IBM-compatible Pentium computer interfaced to the amplifier by a Digidata 1200A acquisition board (Axon Instruments). The generation of voltage-clamp pulses and data acquisition were controlled with pClamp 6.03 software (Axon Instruments).

2.3. Solutions and drugs

The internal pipette solution contained 140 mM KCl, 1 mM $CaCl_2$, 1 mM $MgCl_2$, 25 mM HEPES, and 10 mM EGTA, and was adjusted to pH 7.3 with KOH. The bath solution contained 140 mM NaCl, 5 mM KCl, 1 mM $CaCl_2$, 1 mM $MgCl_2$, 15 mM HEPES, and 10 mM glucose, and was adjusted to pH 7.3 with NaOH. In experiments involving genistein (Calbiochem), a bath solution containing 10 μ M genistein was used for recording the control rKv1.5 currents. EGCG (Calbiochem) and sodium orthovanadate (Calbiochem) were dissolved in distilled water to make 50 mM stock solutions. Chelerythrine (Research Biochemicals International) and genistein were dissolved in dimethyl sulfoxide (DMSO) to make stock solutions of 10 and 50 mM, respectively. The final concentration of DMSO was less than 0.1%, and at this concentration, DMSO had no effect on rKv1.5 currents.

2.4. Data analysis

Data were analyzed using Origin 6.0 software (Microcal Software, Inc.). The concentration-dependent curve for current inhibition by EGCG was fitted to the Hill equation:

$$I(\%) = 1 / \{1 + (IC_{50}/[D])^n\} \quad (1)$$

in which $I(\%)$ is the percentage current inhibition ($I(\%) = [1 - I_{\text{drug}}/I_{\text{control}}] \times 100$) at the test potential; IC_{50} is the inhibitory concentration 50%, the concentration at which inhibition is half-maximal; n is the Hill coefficient; and $[D]$ represents various drug concentrations. Activation curves were fitted with the Boltzmann equation:

$$y = 1 / \{1 + \exp(-(V - V_{1/2})/k)\} \quad (2)$$

where k represents the slope factor; V the test potential; and $V_{1/2}$ the potential at which the conductance is half-maximal. The steady-state voltage-dependence of inactivation was investigated using a double pulse voltage protocol. Currents

were measured using a 250-msec depolarizing pulse of +50 mV, while 20-sec preconditioning pulses were varied from –60 to +10 mV by increments of 10 mV, in the absence and presence of drugs. The experimental points were calculated as shown in equation 3a:

$$\text{Normalized } I = (I - I_c) / (I_{\max} - I_c) \quad (3a)$$

in which I_{\max} represents the current measured at the most hyperpolarized preconditioning pulse, and I_c represents a non-zero current that is not inactivated at the most depolarized 20-sec preconditioning pulse. We eliminated this non-zero residual current by subtracting it from the actual value. The resulting steady-state inactivation data were fitted with the Boltzmann equation:

$$y = 1 / \{1 + \exp(V - V_{1/2}) / k\} \quad (3b)$$

where V is the preconditioning potential; $V_{1/2}$ represents the potential corresponding to the half-inactivation point; and k represents the slope factor. The activation and deactivation kinetics were determined by fitting the sum of the exponentials:

$$y = B + A_1 \exp(-t/\tau_1) + A_2 \exp(-t/\tau_2) + \dots + A_n \exp(-t/\tau_n) \quad (4)$$

in which τ_1 , τ_2 , and τ_n are the time constants; A_1 , A_2 , and A_n are the amplitudes of each component of the exponential; and B is the baseline value.

Data are expressed as means \pm SEM. Student's t -test and ANOVA were used for statistical analysis. Statistical significance was assumed when $P < 0.05$.

3. Results

3.1. Concentration-dependent inhibition of rKv1.5 by EGCG

In whole-cell configurations, no voltage-gated current was detected in untransfected CHO cells, as described previously [19]. Fig. 1A shows the effectiveness of different EGCG concentrations on rKv1.5 currents when rKv1.5 was expressed in CHO cells. Under control conditions, rKv1.5 currents were characterized by rapid activation and then slow inactivation while a depolarizing pulse was maintained, as described previously [16]. The onset of drug action was relatively slow. When bath perfusion was switched to solutions containing different concentrations of EGCG, inhibition of rKv1.5 reached a steady state within 8 min. The washout was also slow and incomplete. The washout of EGCG by the perfusion of drug-free solution was achieved within 6 min, and currents recovered to $64.0 \pm 2.1\%$ ($N = 8$). EGCG inhibition was characterized both by a slowing of the apparent rate of activation and by a reduction in peak current amplitude in a concentration-dependent

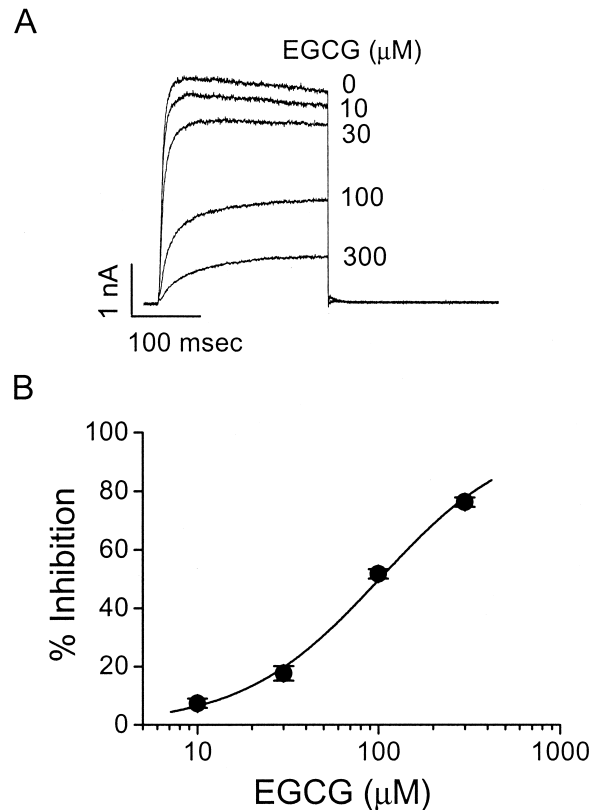


Fig. 1. Concentration-dependence of EGCG-induced inhibition of rKv1.5 currents expressed in CHO cells. (A) Superimposed current traces were produced by applying 250-msec depolarizing pulses from a holding potential of –80 to +50 mV every 20 sec in the absence and presence of 10, 30, 100, and 300 μ M EGCG, as indicated. (B) Concentration-dependent curve of inhibition by EGCG. Peak amplitudes of rKv1.5 currents during the series of depolarizing pulses were used as an index of inhibition, and percentage inhibition was plotted against various concentrations of EGCG. The solid line is fitted to the data points by the Hill equation, which yielded an IC_{50} of $101.2 \pm 6.2 \mu$ M and a Hill coefficient of 1.2 ± 0.1 ($N = 5$). Data are expressed as means \pm SEM.

manner. To determine the concentration-dependence of EGCG action on rKv1.5, we took the effects of EGCG on the peak amplitude of rKv1.5 currents at a 250-msec depolarizing pulse of +50 mV to reflect the drug effects on rKv1.5. In Fig. 1B, a non-linear least-squares fit of the Hill equation to the concentration-response data, which correspond to the percentage inhibition of the current, yielded an apparent IC_{50} of $101.2 \pm 6.2 \mu$ M and a Hill coefficient of 1.2 ± 0.1 ($N = 5$). The value of the Hill coefficient suggests that one molecule of EGCG is sufficient to inhibit a single rKv1.5 channel.

3.2. Effects of protein kinase inhibitors on rKv1.5 inhibition by EGCG

We tested whether the inhibition of rKv1.5 by EGCG is mediated through signal transduction pathways by using PTK inhibitors (genistein, AG1296), a protein tyrosine

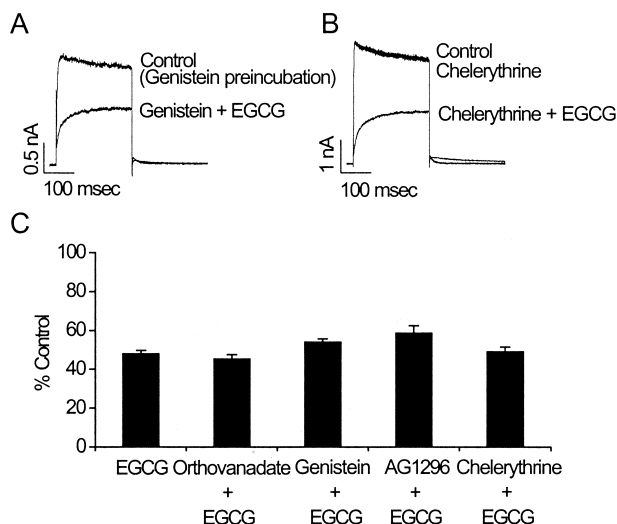


Fig. 2. Different protein kinase inhibitors do not affect the inhibition of rKv1.5 by EGCG. Superimposed original currents were produced by applying 250-msec depolarizing pulses from a holding potential of -80 to $+50$ mV every 20 sec. (A) The control current, recorded after a 1-hr preincubation with $10 \mu\text{M}$ genistein, and the current measured after a further 8-min treatment with $100 \mu\text{M}$ EGCG, are shown. For this experiment, a bath solution containing $10 \mu\text{M}$ genistein was used. (B) The control current, the current recorded after a 5-min exposure to $10 \mu\text{M}$ chelerythrine, and the current measured after an 8-min treatment with $100 \mu\text{M}$ EGCG, are shown. The same protocol was used for cells treated with $100 \mu\text{M}$ AG1296 and $500 \mu\text{M}$ sodium orthovanadate (original current traces are not shown). (C) Peak amplitudes of rKv1.5 currents during 250-msec depolarizing pulses under each set of experimental conditions (A, B) were normalized to that of the control currents, and displayed as the percentage inhibition to show the effects of genistein, AG1296, sodium orthovanadate, chelerythrine, and EGCG. Data are expressed as means \pm SEM ($N > 3$).

phosphatase inhibitor (sodium orthovanadate), and a PKC inhibitor (chelerythrine). Preincubation with genistein had no effect on the activation or inactivation kinetics of rKv1.5 compared with control currents (Fig. 2A). Addition of $100 \mu\text{M}$ EGCG to a bath solution containing $10 \mu\text{M}$ genistein caused the peak amplitude of the rKv1.5 current to decrease by $45.9 \pm 2.6\%$ ($N = 4$). The effects of chelerythrine on the inhibition of rKv1.5 by EGCG are shown in Fig. 2B. A 5-min exposure to $10 \mu\text{M}$ chelerythrine did not inhibit rKv1.5. After a 5-min exposure to chelerythrine, EGCG inhibited the peak amplitude of the rKv1.5 current by $50.8 \pm 2.3\%$ ($N = 3$). A similar series of experiments with sodium orthovanadate and AG1296 resulted in EGCG-induced inhibition of rKv1.5 by $54.6 \pm 2.3\%$ ($N = 3$) and $41.2 \pm 4.5\%$ ($N = 4$), respectively. From the summary of results (Fig. 2C), values for the inhibition by EGCG of the rKv1.5 peak currents were not significantly different after pretreatment with various inhibitors from the inhibition induced by EGCG alone in the control bath solution. These results strongly suggest that EGCG inhibited rKv1.5 currents, not through a signal transduction pathway, but by direct interaction with rKv1.5.

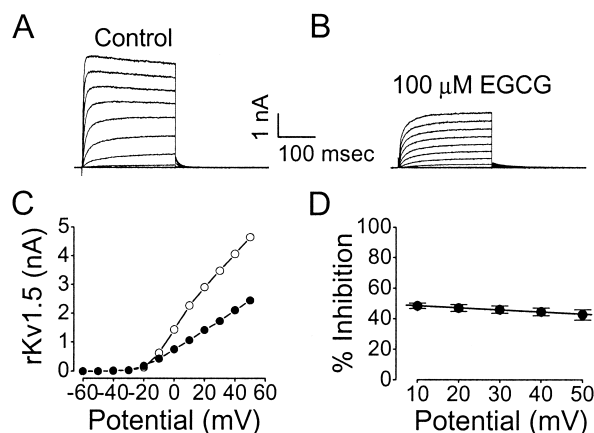


Fig. 3. Inhibition of rKv1.5 currents by EGCG is independent of voltage. rKv1.5 currents were produced by applying 250-msec depolarizing pulses from -60 to $+50$ mV in 10-mV increments every 10 sec, from a holding potential of -80 mV. The original current traces under control conditions and after the addition of $100 \mu\text{M}$ EGCG are shown in (A) and (B), respectively. (C) Resultant I-V relationships taken from the peak amplitudes of rKv1.5 currents (\circ , control; \bullet , $100 \mu\text{M}$ EGCG). (D) Percentage inhibition from data in (C). Data are expressed as means \pm SEM ($N = 5$).

3.3. Voltage-independence of rKv1.5 inhibition by EGCG

Fig. 3 shows the effects of EGCG on the relationship between current and voltage (I-V). Original current traces under control conditions (Fig. 3A) and after the addition of $100 \mu\text{M}$ EGCG (Fig. 3B) are shown. Fig. 3C was constructed by plotting the peak amplitude of the rKv1.5 current as a function of the test pulse potential. Inhibition of the peak current was observed for the entire voltage range over which rKv1.5 was activated. When current inhibition was expressed as a function of test potential, EGCG-induced inhibition of rKv1.5 currents was voltage-independent across the voltage range (from $+10$ to $+50$ mV) over which rKv1.5 was fully activated. For example, at a test potential of $+10$ mV, EGCG inhibited rKv1.5 currents by $48.4 \pm 1.9\%$, whereas at $+50$ mV, inhibition was $42.7 \pm 3.4\%$ ($N = 5$). Least-squares linear regression of the data (Fig. 3D) yielded a value approximately equal to zero for the slope of the line.

3.4. Effect of EGCG on the steady-state activation and inactivation of rKv1.5

The potential ($V_{1/2}$) of the half-activation point and the slope factor (k) of the steady-state activation curves were -5.1 ± 0.8 mV and 5.7 ± 0.5 mV, respectively, for the control, and -5.7 ± 1.0 mV and 7.6 ± 0.7 mV, respectively, for cells treated with $100 \mu\text{M}$ EGCG ($N = 5$, Fig. 4). EGCG had no effect on the voltage-dependence of activation. Similarly, EGCG had no effect on the voltage-dependence of steady-state inactivation. $V_{1/2}$ and k were -24.3 ± 0.5 mV and 3.5 ± 0.3 mV, respectively, for the control, and -24.7 ± 0.5 mV and 6.7 ± 0.3 mV, respectively, in the presence of EGCG ($N = 4$).

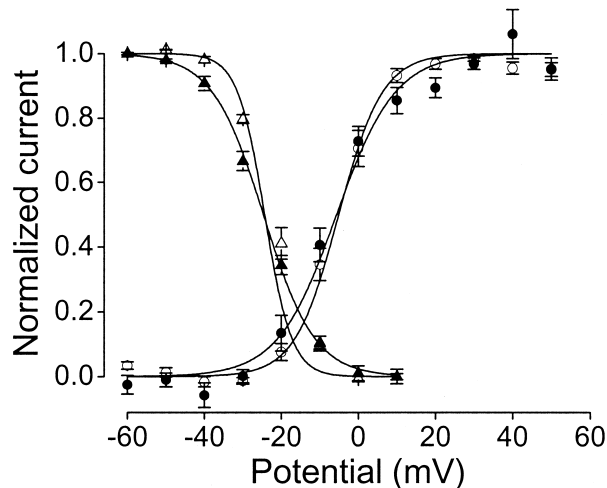


Fig. 4. Voltage-dependence of the steady-state activation and inactivation of rKv1.5 currents in the absence (\circ , Δ , \square) and presence (\bullet , \blacktriangle , \blacksquare) of 100 μ M EGCG. The steady-state activation curves were obtained from tail current amplitudes immediately after the capacitive transient. The tail currents were obtained at -40 mV after 250-msec depolarizing pulses from -60 to $+50$ mV, and were normalized to their maximal value before each set of data was fitted to equation 2. The steady-state inactivation curves were obtained using a typical double pulse protocol followed by normalization, fitting each set of data to equations 3a and 3b (for details, see Materials and methods). Data are expressed as means \pm SEM ($N > 4$).

3.5. Effect of EGCG on the ion selectivity of rKv1.5

The ion selectivity of the rKv1.5 channel was examined by measuring the reversal potential of tail currents in the absence and presence of 100 μ M EGCG. The reversal potential of rKv1.5 under control conditions was about -70 mV, and was not affected by EGCG (Fig. 5).

3.6. Effects of EGCG on activation and deactivation kinetics

Original current traces obtained in the absence and presence of 100 μ M EGCG were superimposed, and clearly

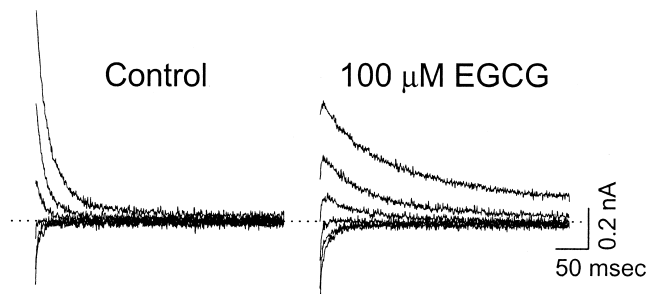


Fig. 5. EGCG has no effect on the reversal potential of rKv1.5 currents. The reversal potential of rKv1.5 was recorded by the following double pulse protocol. A prepulse consisting of a 250-msec depolarizing pulse of $+50$ mV from a holding potential of -80 mV was followed by 250-msec repolarizing pulses in 10-mV increments from -90 to -40 mV. Each pulse was applied after an interval of 30 sec. The original current traces in the absence and presence of 100 μ M EGCG are shown. The dotted line represents a zero current.

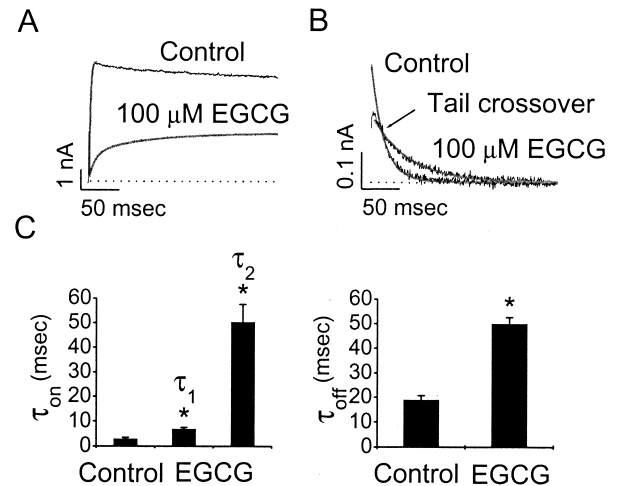


Fig. 6. Effects of EGCG on activation and deactivation kinetics. (A) Superimposed original current traces produced by a 250-msec depolarizing pulse of $+50$ mV from a holding potential of -80 mV, under control conditions and in the presence of 100 μ M EGCG. The solid lines over the current traces are monoexponential and biexponential least-squares fits of the data for the activation of rKv1.5 in the absence and presence of 100 μ M EGCG, respectively. The dotted line represents a zero current. (B) Tail currents were recorded during a 250-msec repolarizing pulse of -40 mV after a 250-msec depolarizing pulse of $+50$ mV from a holding potential of -80 mV, in the absence and presence of 100 μ M EGCG. When the two tail currents in the absence and presence of EGCG were superimposed, a tail crossover phenomenon (indicated by the arrow) was observed. The solid lines over the current traces represent the monoexponential least-squares fit of the data for deactivation of rKv1.5, in the absence and presence of 100 μ M EGCG. (C) Summary data obtained from A (left panel) and B (right panel). τ_{on} and τ_{off} represent the activation and deactivation time constants, respectively. The symbol * indicates a statistically significant difference ($N > 5$, $P < 0.05$). Data are expressed as means \pm SEM.

showed that the period of onset of activation of the current produced by a 250-msec depolarizing pulse of $+50$ mV was extended by EGCG (Fig. 6A and 6C). Under control conditions, channel activation at $+50$ mV was well fitted by a monoexponential function immediately after the transient capacitive current on depolarizing pulses. This process yielded a time constant (τ) for an activation of 2.9 ± 0.6 msec ($N = 5$). In contrast, in the presence of 100 μ M EGCG, the current trace was better fitted by a biexponential function that yielded two time constants for activation. The calculated values of τ_1 and τ_2 were 6.9 ± 0.6 msec and 50.3 ± 7.2 msec, respectively, ($N = 5$). The significant increase in the two activation time constants compared with control values ($P < 0.05$) indicates that the activation kinetics was significantly modified by EGCG. Original tail current traces produced by a 250-msec repolarizing return pulse of -40 mV after a 250-msec depolarizing pulse of $+50$ mV from a holding potential of -80 mV, under control conditions and in the presence of 100 μ M EGCG, were superimposed, and are well fitted by a monoexponential function, as shown in Fig. 6B and 6C. Under control conditions, the tail current was completely deactivated with a time constant of 19.0 ± 1.8 msec ($N = 8$). In the presence

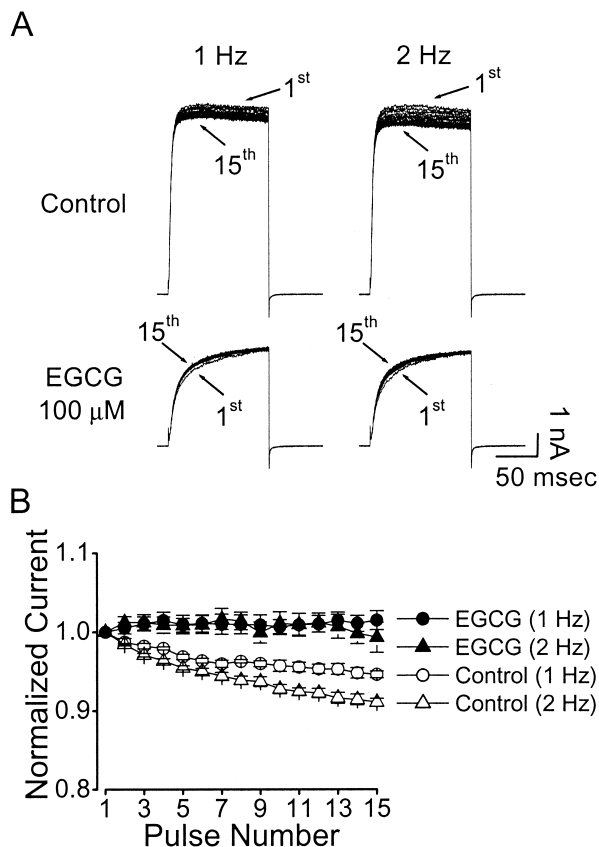


Fig. 7. (A) Effects of repetitive depolarization on EGCG-induced inhibition of rKv1.5 currents. Repetitive depolarizing pulses (125 msec) from a holding potential of -80 mV to $+50$ mV were applied at two different frequencies, 1 and 2 Hz, under control conditions ($N = 5$) and in the presence of $100 \mu\text{M}$ EGCG ($N = 6$). (B) The peak amplitudes of currents at each pulse were normalized to the peak amplitudes of currents obtained at the first pulse, and were then plotted against the pulse numbers. Data are expressed as means \pm SEM.

of $100 \mu\text{M}$ EGCG, the initial peak amplitude of the tail current decreased, and the subsequent decline in the current was significantly slowed, with a deactivation time constant of 50.0 ± 2.7 msec ($N = 8$, $P < 0.05$), which resulted in a tail crossover phenomenon.

3.7. Evidence for the reversal of inhibition on depolarization

Original current traces, in the absence and presence of $100 \mu\text{M}$ EGCG, were obtained by 15 repetitive applications of depolarizing pulses at two different frequencies, 1 Hz and 2 Hz (Fig. 7A). Under control conditions, the peak amplitude of the rKv1.5 current decreased slightly, by $5.4 \pm 0.4\%$ ($N = 5$), at a frequency of 1 Hz, and by $8.9 \pm 0.5\%$ ($N = 5$) at a frequency of 2 Hz, in a weakly frequency-dependent manner (Fig. 7B). In the presence of $100 \mu\text{M}$ EGCG, there was a reduction in peak amplitude produced by the first depolarizing pulse. This reduction averaged $49.2 \pm 1.7\%$ ($N = 6$). Thereafter, during the application of the series of

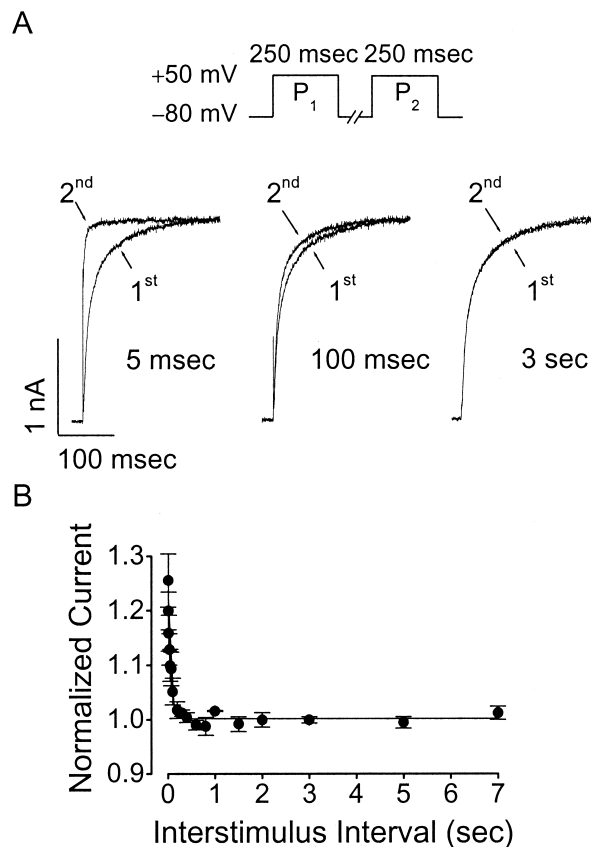


Fig. 8. Reversal of inhibition and reinhibition of rKv1.5 channels by EGCG. A double pulse protocol, with pulses separated by various time intervals, was applied. The first pulse (P_1), a 250-msec depolarizing pulse of $+50$ mV from a holding potential of -80 mV, was followed by a second identical pulse (P_2) after increasing time intervals from 5 msec to 7000 msec at -80 mV. Each pulse was applied after an interval of 30 sec. (A) Superimposed original current traces produced by P_1 and P_2 for 5, 100, and 3000 msec interpulse intervals. (B) Time-course of reinhibition by $100 \mu\text{M}$ EGCG. The current amplitudes measured at 36 msec after the start of P_2 were normalized against those measured at 36 msec after the start of P_1 , and plotted as a function of the various interpulse intervals. Each data point was obtained in the presence of $100 \mu\text{M}$ EGCG (\bullet) ($N = 6$). Data are expressed as means \pm SEM.

pulses, the current amplitude was almost unaffected when measured at the end of the pulse at frequencies of 1 Hz and 2 Hz. Moreover, the amplitude of the rKv1.5 current increased slightly, and this increase was apparent at approximately 36 msec after the start of the depolarization pulses. These results suggest that there is little use-dependence of EGCG action, and repetitive depolarization reversed the reduction in amplitude during the early part of the pulse.

To further examine the reversal of the inhibition induced by EGCG, the next experiment was carried out using identical double pulses with various intervals between the first (P_1) and second (P_2) pulses. Fig. 8A shows the original current traces for 5, 100, and 3000 msec interpulse intervals in the presence of $100 \mu\text{M}$ EGCG. For short interpulse intervals (5 msec), currents produced by P_2 show a fast rising phase similar to the control currents recorded in the absence of EGCG, which indicates the reversal of inhibi-

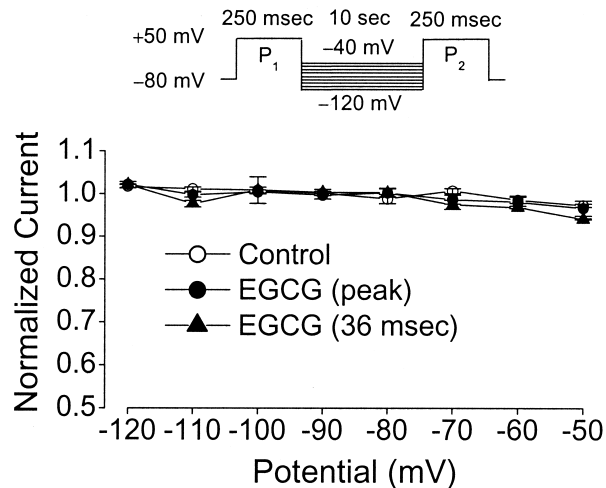


Fig. 9. Effect of EGCG on the multiple closed states of rKv1.5. A double pulse protocol was applied. The first pulse (P_1), a 250-msec depolarizing pulse of +50 mV from a holding potential of -80 mV, was followed by a second identical pulse after a 10-sec repolarization step to various potentials from -120 to -40 mV, in 10-mV increments. Each pulse was applied after an interval of 30 sec. The peak current amplitudes during P_1 (○, control; ●, 100 μ M EGCG) or the current amplitudes at 36 msec after the start of P_1 (▲, 100 μ M EGCG) were normalized against the respective current amplitudes obtained during P_2 or after the start of P_2 , and plotted as a function of various repolarizing pulses. Data are expressed as means \pm SEM ($N = 4$).

tion. As interpulse intervals increase, the two currents produced by P_1 and P_2 are identical, which suggests that the reversal of inhibition was abolished and a significant amount of inhibition of rKv1.5 by EGCG must be re-established during the interpulse interval, when channels are in the closed state (Fig. 8B) [20,21]. The reversal of inhibition indicated in Figs. 7 and 8 strongly suggests that EGCG preferentially interacts with the closed state and unbinds during the active state of rKv1.5 channels.

3.8. Effect of EGCG on the multiple closed state of rKv1.5

Like human Kv1.5, which has been more thoroughly studied [22], the rKv1.5 channel is thought to have multiple closed states, and the transitions between these states are voltage-dependent. We further tested whether the potency of EGCG-induced inhibition of rKv1.5 is dependent on multiple closed states of the channel. If the affinity between EGCG and the rKv1.5 channel is dependent on multiple closed states of rKv1.5, then the potency of EGCG-induced inhibition will be different at various holding potentials because the size of the populations of various closed states are dependent on the holding potentials. Normalized currents did not significantly change under control conditions or in the presence of EGCG, over potentials between -120 mV and -50 mV (Fig. 9), which are negative to the threshold of rKv1.5 channel activation (Fig. 3C). The ANOVA shows no significant difference among these groups. These

results suggest that the potency of EGCG-induced inhibition of rKv1.5 is not dependent on various closed states of the channel, indicating that the affinity for all the closed states of rKv1.5 is identical.

4. Discussion

The present results show that EGCG, the main constituent of green tea, directly inhibits rKv1.5 channels in a concentration-dependent manner and independently of signal transduction pathways. Demonstration of the direct inhibition of rKv1.5 by EGCG is the first evidence for the action of this compound on ion channels.

EGCG selectively inhibits the tyrosine phosphorylation of PDGF-R β [13], the PTK activities of epidermal growth factor receptor, PDGF receptor, and fibroblast growth factor receptor [23], and PKC [24]. Therefore, it is possible that EGCG can indirectly inhibit rKv1.5 currents through signal transduction pathways. Furthermore, the rKv1.5 channel has multiple consensus sites for phosphorylation by various protein kinases [17,25], and can be strongly modulated through phosphorylation-dependent signal transduction pathways [26,27]. Our results suggest that inhibition of rKv1.5 currents by EGCG does not involve a phosphorylation-dependent signal transduction pathway. However, we do not completely rule out an indirect mechanism of action through a yet-to-be-determined transduction system.

An important observation in the present study is that the monoexponential rise of Kv1.5 currents was reshaped to a double exponential in the presence of EGCG. In other words, EGCG caused a marked slowing of the apparent current activation. One possible explanation for the slowing of the activation kinetics is that the steady-state activation curve of rKv1.5 by EGCG is shifted equally. However, this is not likely to be the case in our experiment. The steady-state activation curve was not affected by EGCG. The results of this study with EGCG are similar to those of a previous study on the inhibition of neuronal Kv1.1 currents by fluoxetine [28], and are characteristic of inhibition induced by an ion channel blocker that binds channels in the closed state [20,29]. Furthermore, the lack of effect of EGCG on the voltage-dependence of the steady-state inactivation suggests that EGCG does not interact with the inactivated conformation of rKv1.5 channels.

A pore blocker usually exhibits use-dependent blockage of a channel. However, in our experiment, use-dependent inhibition by EGCG was not observed (Fig. 7). In contrast, repetitive depolarization induced the reversal of inhibition during the early part of the activating pulse. Furthermore, a reversal of inhibition was clearly produced by identical double pulses with various intervals between the first and second pulse: the shorter the interval, the greater the reversal of inhibition. This result agrees well with a previous report [30,31], which showed that repetitive depolarizing pulses reversed the block in a manner dependent on the

duration and interval of pulses. These results suggest that EGCG inhibits rKv1.5 through a preferential interaction with the closed state of the channel, and that inhibition may be reversed by opening the channel at positive potentials. Other evidence favoring closed-channel binding includes the voltage-independent effects of EGCG on rKv1.5 at potentials positive to 0 mV, when channel activation reached saturation. This explanation could be applied to EGCG, because EGCG is predominately in an uncharged form at physiological pH (pH = 7.3), resulting in independence of the transmembrane electric field. In this situation, we expect the voltage to be independent of the action of the drug. In general, open channel blocking mechanisms are associated with the charged form of drug molecules and a voltage-dependence of the block [32,33]. This analysis suggests that EGCG is unlikely to be an open channel blocker for rKv1.5.

The fact that EGCG slowed the time-course of deactivating tail currents, thus inducing a crossover phenomenon, does not support a closed-channel binding mechanism. The effect of EGCG on the tail current was surprising. EGCG produced a paradoxical effect of tail crossover, which is usually observed in open channel blocks [16,32–34]. The effects of EGCG on rKv1.5 may be complex, and it is unlikely that inhibition can be accounted for by a simple closed-channel blocking mechanism. Furthermore, at short interpulse intervals (5 msec), the current produced by the second pulse shows fast activation kinetics, similar to those of the control (Fig. 8). At the end of the pulse, however, both the first and second current traces were the same amplitude. Thus, repetitive depolarization could reverse the reduced amplitude during the early part of the pulse and the slowing of the activation kinetics, but not the reduced amplitude at the end of pulse. Shortening the interpulse interval only impedes the binding to the closed state, and therefore facilitates the activation. However, the pore block effect cannot be reversed during depolarization. This explains, at least partly, why the current amplitude does not recover during repetitive depolarization at the end of the pulse. Therefore, it is likely that the inhibition of rKv1.5 by EGCG includes at least two effects: the drug binds to channels in the closed state to slow activation, and also blocks the channels by pore occlusion while depolarization is maintained. However, an alternative explanation for tail crossover and the slowing of activation could be that the binding of EGCG to the closed state alone produces a large energy barrier to bidirectional transitions between the closed and open states, thereby slowing both the opening and the closing rates.

We do not know the exact mechanism by which EGCG inhibits rKv1.5 channels. EGCG is known to bind to several proteins, and affects the activity of enzymes and receptors [35,36]. One possibility is that EGCG interacts directly with the channel protein to alter the probability of channel opening, or the gating kinetics. However, it is equally possible

that this compound binds to biological membranes via channel proteins, and affects ion channels allosterically.

This study is the first to investigate the direct effects of EGCG on ion channels, specifically cloned rKv1.5 channels. Although green tea is reported to have many beneficial biological functions, there are only a few articles concerning the molecular mechanisms of its action [12,13,23]. Therefore, our results suggesting a direct inhibition of ion channels (rKv1.5) by EGCG will provide a critical clue in elucidating the molecular mechanisms for the various functions of green tea. However, it should be noted that the EGCG concentrations used in this study are much higher than the anticipated plasma concentrations in humans. After drinking five cups of green tea, peak plasma levels of EGCG average about 1 μ M [37]. Although it is difficult to be certain of the clinical significance of the inhibitory effects of EGCG on rKv1.5, these effects of EGCG are interesting and provide insight into the mechanisms of action of this class of compounds on ion channels.

In conclusion, our data suggest that EGCG directly interacts with multiple states of the rKv1.5 channel, and that EGCG-induced inhibition is reversed during membrane depolarization.

Acknowledgments

We thank Dr. Leonard Kaczmarek (Yale University School of Medicine, USA) for the rKv1.5 cDNA and Won Kim for reading the manuscript. This work was supported by a Korea Research Foundation Grant (KRF-2000-015-FP0026).

References

- [1] De Whalley CV, Rankin SM, Hoult JR, Jessup W, Leake DS. Flavonoids inhibit the oxidative modification of low density lipoproteins by macrophages. *Biochem Pharmacol* 1990;39:1743–50.
- [2] Tijburg LB, Mattern T, Folts JD, Weigerber UM, Katan MB. Tea flavonoids and cardiovascular diseases. *Crit Rev Food Sci* 1997;37:771–85.
- [3] Han C. Screening of anticarcinogenic ingredients in tea polyphenols. *Cancer Lett* 1997;114:153–8.
- [4] Nakachi K, Suemasu K, Suga K, Takeo T, Imai K, Higashi Y. Influence of drinking green tea on breast cancer malignancy among Japanese patients. *Jpn J Cancer Res* 1998;89:254–61.
- [5] Dashwood RH, Xu M, Hernaez JF, Hasaniya N, Youn K, Razzuk A. Cancer chemopreventive mechanisms of tea against heterocyclic amine mutagens from cooked meat. *Proc Soc Exp Biol Med* 1999;220:239–43.
- [6] Kuroda Y, Hara Y. Antimutagenic and anticarcinogenic activity of tea polyphenols. *Mutat Res* 1999;436:69–97.
- [7] Kondo K, Kurihara M, Miyata N, Suzuki T, Toyoda M. Scavenging mechanisms of (–)-epigallocatechin gallate and (–)-epicatechin gallate on peroxyl radicals and formation of superoxide during the inhibitory action. *Free Radic Biol Med* 1999;27:855–63.
- [8] Wei H, Zhang X, Zhao JK, Wang ZY, Bickers D, Lebowitz M. Scavenging of hydrogen peroxide and inhibition of ultraviolet light-

- induced oxidative DNA damage by aqueous extracts from green and black teas. *Free Radic Biol Med* 1999;26:1427–35.
- [9] Katiyar SK, Matsui MS, Elmets CA, Mukhtar H. Polyphenolic antioxidant (–)-epigallocatechin-3-gallate from green tea reduces UVB-induced inflammatory responses and infiltration of leukocytes in human skin. *Photochem Photobiol* 1999;69:148–53.
 - [10] Valcic S, Muders A, Jacobsen NE, Liebler DC, Timmermann BN. Antioxidant chemistry of green tea catechins. Identification of products of the reaction of (–)-epigallocatechin gallate with peroxyl radicals. *Chem Res Toxicol* 1999;12:382–6.
 - [11] Balentine DA, Wiseman SA, Bouwens LCM. The chemistry of tea flavonoids. *Crit Rev Food Sci Nutr* 1997;37:693–704.
 - [12] Kitano K, Nam KY, Kimura S, Fujiki H, Imanishi Y. Sealing effects of (–)-epigallocatechin gallate on protein kinase C and protein phosphatase 2A. *Biophys Chem* 1997;65:157–64.
 - [13] Ahn HY, Hadizadeh KR, Seul C, Yun YP, Vetter H, Sachindis A. Epigallocatechin-3 gallate selectively inhibits the PDGF-BB-induced intracellular signaling transduction pathway in vascular smooth muscle cells and inhibits transformation of *sis*-transfected NIH 3T3 fibroblasts and human glioblastoma cells (A172). *Mol Biol Cell* 1999;10:1093–104.
 - [14] Klimatcheva E, Wonderlin WF. An ATP-sensitive K⁺ current that regulates progression through early G1 phase of the cell cycle in MCF-7 human breast cancer cells. *J Membrane Biol* 1999;171:35–46.
 - [15] Yao X, Kwan HY. Activity of voltage-gated K⁺ channels is associated with cell proliferation and Ca²⁺ influx in carcinoma cells of colon cancer. *Life Sci* 1999;65:55–62.
 - [16] Choi BH, Choi JS, Jeong SW, Hahn SJ, Yoon SH, Jo YH, Kim MS. Direct block by bisindolylmaleimide of rat Kv1.5 expressed in Chinese hamster ovary cells. *J Pharmacol Exp Ther* 2000;293:634–40.
 - [17] Swanson R, Marshall J, Smith JS, Williams JB, Boyle MB, Folander K, Luneau CJ, Antanavage J, Oliva C, Buhrow SA, Bennett C, Stein RB, Kaczmarek LK. Cloning and expression of cDNA and genomic clones encoding three delayed rectifier potassium channels in rat brain. *Neuron* 1990;4:929–39.
 - [18] Hamill OP, Marty A, Neher E, Sakmann B, Sigworth FJ. Improved patch-clamp techniques for high-resolution current recording from cells and cell-free membrane patches. *Pflügers Arch* 1981;391:85–100.
 - [19] Philipson LH, Malayev A, Kuznetsov A, Chang C, Nelson DJ. Functional and biochemical characterization of the human potassium channel Kv1.5 with a transplanted carboxyl-terminal epitope in stable mammalian cell lines. *Biochim Biophys Acta* 1993;1153:111–21.
 - [20] Campbell DL, Qu Y, Rasmusson RL, Strauss HC. The calcium-independent transient outward potassium current in isolated ferret right ventricular myocytes. II. Closed state reverse use-dependent block by 4-aminopyridine. *J Gen Physiol* 1993;101:603–26.
 - [21] Bouchard R, Fedida, D. Closed- and open-state binding of 4-aminopyridine to the cloned human potassium channel Kv1.5. *J Pharmacol Exp Ther* 1995;275:864–76.
 - [22] Zagotta WN, Hoshi T, Dittman J, Aldrich RW. *Shaker* potassium channel gating II: Transitions in the activation pathway. *J Gen Physiol* 1994;103:279–319.
 - [23] Yu-Chih L, Shoen-Yn LS, Chieh-Fu C, Jen-Kun L. Suppression of extracellular signals and cell proliferation through EGF receptor binding by (–)-epigallocatechin gallate in human A431 epidermoid carcinoma cells. *J Cell Biochem* 1997;67:55–65.
 - [24] Komori A, Yatsunami J, Okabe S, Abe S, Hara K, Suganuma M, Kim SJ, Fujiki H. Anticarcinogenic activity of green tea polyphenols. *Jpn J Clin Oncol* 1993;23:186–90.
 - [25] Tseng-Crank JCL, Tseng GN, Schwartz A, Tanouye MA. Molecular cloning and functional expression of a potassium channel cDNA isolated from a rat cardiac library. *FEBS Lett* 1990;268:63–8.
 - [26] Uebele VN, Yeola SW, Snyders DJ, Tamkun MM. Deletion of highly conserved C-terminal sequences in the Kv1 K⁺ channel sub-family does not prevent expression of currents with wild-type characteristics. *FEBS Lett* 1994;340:104–8.
 - [27] Li GR, Feng JL, Wang ZG, Fermini B, Nattel S. Adrenergic modulation of ultrarapid delayed rectifier K⁺ current in human atrial myocytes. *Circ Res* 1996;78:903–15.
 - [28] Tytgat J, Maertens CH, Daenens P. Effects of fluoxetine on a neuronal, voltage-dependent potassium channel (Kv1.1). *Br J Pharmacol* 1997;122:1417–24.
 - [29] Remillard CV, Leblanc N. Mechanism of inhibition of delayed rectifier K⁺ current by 4-aminopyridine in rabbit coronary myocytes. *J Physiol* 1996;491:383–400.
 - [30] Yeh JZ, Oxford GS, Wu CH, Narahashi T. Dynamics of aminopyridine block of potassium channels in squid axon membrane. *J Gen Physiol* 1976;68:519–35.
 - [31] Kirsch GE, Yeh JZ, Oxford GS. Modulation of aminopyridine block of potassium currents in squid axon. *Biophys J* 1986;50:637–44.
 - [32] Valenzuela C, Delpon E, Franqueza L, Gay P, Perez O, Tarmago J, Snyders DJ. Class III antiarrhythmic effects of zatebradine: time-, state-, use-, and voltage-dependent block of hKv1.5 channels. *Circulation* 1996;94:562–70.
 - [33] Choi JS, Hahn SJ, Rhie DJ, Jo YH, Kim MS. Mechanism of fluoxetine block of cloned voltage-activated potassium channel Kv1.3. *J Pharmacol Exp Ther* 1999;291:1–6.
 - [34] Choi JS, Hahn SJ, Rhie DJ, Jo YH, Kim MS. Staurosporine directly blocks Kv1.3 channels expressed in Chinese hamster ovary cells. *Naunyn-Schmiedeberg's Arch Pharmacol* 1999;359:256–61.
 - [35] Haslam E. Natural polyphenols and vegetable tannins as drugs: possible modes of action. *J Nat Prod* 1996;59:205–15.
 - [36] Lin YL, Lin JK. (–)-Epigallocatechin-3-gallate blocks the induction of nitric oxide synthase by down-regulating lipopolysaccharide-induced activity of transcription factor nuclear factor- κ B. *Mol Pharmacol* 1997;52:465–72.
 - [37] Yang CS, Chen L, Lee MJ, Balentine D, Kuo MC, Schantz SP. Blood and urine levels of tea catechins after ingestion of different amounts of green tea by human volunteers. *Cancer Epidemiol Biomarkers Prev* 1998;7:351–4.